Mechanical Anisotropy of Semicrystalline Polymer in Relation to Molecular Orientation*

By

Hiromichi KAWAI**

(Received September 30, 1968)

A brief review on the mechanical anisotropy of crystalline polymers in bulk in relation to the molecular orientations, is presented.

First, a mathematical representation of orientation distribution of structural units within the bulk polymer, is given in terms of an expansion of the distribution function in a series of spherical harmonics. Each coefficient of the expanded series is discussed in relation to several kinds of orientation factors, average degrees of the orientation distribution, defined by different authors independently.

Second, several optical techniques to evaluate the orientation factors, the second and fourth moments of the orientation distribution of crystalline and noncrystalline structural units from the optical dichroic quantities, are discussed. Some experimental results on the orientation behavior of crystalline polymers during uniaxially or biaxially stretching are demonstrated.

Finally, the mechanical anisotropies of oriented crystalline polymers, including uniaxial- and orthogonally biaxial-symmetric systems, are interpreted in terms of the average degrees of orientation distributions of the two kinds of structural units, crystallites and noncrystalline chain segments, and the mechanical anisotropies of the structural units for the glassy state of the polymers; i.e., in terms of the aggregate model of biphase structure on the basis of either the homogeneous stress or strain hypothesis. Furthermore, a modification of the Krigbaum's treatment for the elasticity of the crystalline polymers, which based on the kinetic theory of entropy elasticity, to the anisotropic body, is proposed for the rubbery (or leathery) state of the polymers.

Introduction

The polymer molecules are intrinsically anisotropic in physical properties, such as mechanical and optical ones, which make the bulk properties of polymer aggregates also anisotropic when the polymer molecules are oriented in particular fashions.

This has been successfully used for manufacturing textile fibers and polymer films by means of mechanical drawing or rolling of the polymer aggregates

---

uniaxially or biaxially.   Actually, highly uniaxial or planar orientation of polymer molecules along the fiber axis or film plane can be achieved by the processing, and the mechanical anisotropy to characterize the materials as having high tensile-stiffness with extreme flexibility, results.

In this review, the mechanical anisotropy of crystalline polymer in bulk will be briefly described in quantitative relations to the molecular orientations.

Mathematical Representation of Orientation Distribution Function

Mathematical representation of orientation distribution of structual units within the bulk polymer can be given in terms of an expansion of the distribution function in a series of spherical harmonics,[1),2)] and each coefficient of the expanded series will be discussed in relation to several kinds of orientation factors,[3)] average degrees of orientation distribution, defined by different authors independently.[4−7)]

The orientation of the structural unit within the space of film specimen may be specified by using three Euler angles, ϕ, θ, and η, as shown in Fig. 1. $0-x_1x_2x_3$ is
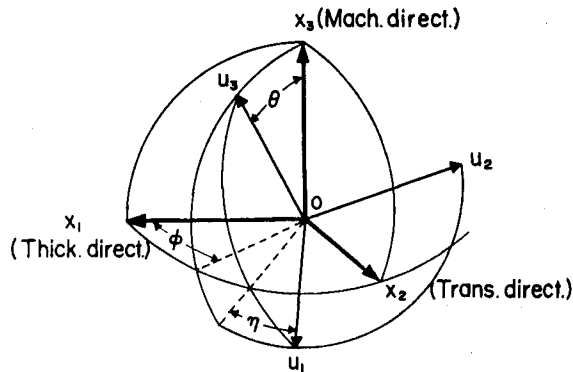

Fig. 1.   Euler angles, ϕ, θ, and η, which specify the orient-
ation of Cartesian coordinates $0-u_1u_2u_3$ fixed within
structural unit with respect to other Cartesian
coordinates $0-x_1x_2x_3$ fixed within the space of film
specimen.

Cartesian coordinates fixed within the space with the x_3 axis being along the stretching direction, and the x_3x_2 plane being parallel to the surface of the specimen. $0-u_1u_2u_3$ is other Cartesian coordinates fixed within the structural unit, where the u_3 axis may be taken as being the polymer chain direction.   The angles θ and ϕ, which define the orientation of u_3 axis of the unit within the space, are the polar and azimuthal angles, respectively, and η specifies the rotation of the unit around its own u_3 axis.

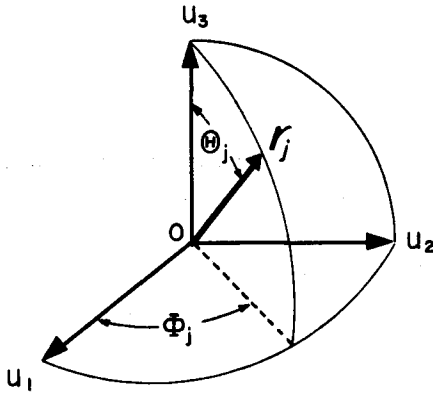Let us consider, as shown in Fig. 2, a given jth axis r_j within the unit being

Fig. 2. Angles Θ_j and Φ_j specify the orient-
ation of a given jth axis of the structural
unit with respect to the Cartesian co-
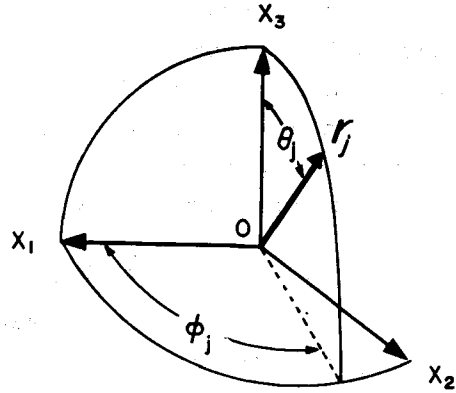ordinates $0-u_1u_2u_3$ fixed within the struc-
tural unit.

Fig. 3. Angles θ_j and ϕ_j specify the orientation
of the given jth axis of the structural unit
with respect to the Cartesian coordinates
$0-x_1x_2x_3$ fixed within the space of film
specimen.

specified by the polar angle Θ_j and the azimuthal angle Φ_j with respect to the
Cartesian coordinates $0-u_1u_2u_3$ of the unit. Similarly, the orientation of the jth
axis with respect to the bulk coordinates $0-x_1x_2x_3$ is given, as shown in Fig. 3, by the
polar angle θ_j and the azimuthal angle ϕ_j. The two sets of angles (Θ_j, Φ_j) and
(θ_j, ϕ_j) referring to the identical axis r_j may be related to each other through
the following equations, which describe a linear transformation of Cartesian coor-
dinates being accompanied by the rotation of coordinate axes by ϕ, θ, and η.

$$\begin{vmatrix} \cos\theta_j \\ \sin\theta_j\cos\phi_j \\ \sin\theta_j\sin\phi_j \end{vmatrix} = T(\theta,\phi,\eta)\begin{vmatrix} \cos\Theta_j \\ \sin\Theta_j\cos\Phi_j \\ \sin\Theta_j\sin\Phi_j \end{vmatrix} \tag{1}$$

where $T(\theta, \phi, \eta)$ is a linear transformation operator given by the following second-
order matrix.

$$T(\theta,\phi,\eta) = \begin{vmatrix} \cos\theta, & -\sin\theta\cos\phi, & \sin\theta\sin\eta, \\ \sin\theta\cos\phi, & \cos\theta\cos\phi\cos\eta & -\cos\theta\cos\phi\sin\eta \\ & -\sin\phi\sin\eta, & -\sin\phi\cos\eta, \\ \sin\theta\sin\phi, & \cos\theta\sin\phi\cos\eta & -\cos\theta\sin\phi\sin\eta \\ & +\cos\phi\sin\eta, & +\cos\phi\cos\eta, \end{vmatrix} \tag{2}$$

The normalized orientation distribution function of the units within the bulk
specimen, $p(\theta, \phi, \eta)$ may be defined by

$$\int_{\eta=0}^{2\pi}\int_{\phi=0}^{2\pi}\int_{\theta=0}^{\pi} [p(\theta,\phi,\eta)\sin\theta]\,d\theta\,d\phi\,d\eta = 1. \tag{3}$$

Similarily, the normalized orientation distribution function of the jth axis, $q^j(\theta_j, \phi_j)$ may be defined by

$$\int_{\phi_j=0}^{2\pi} \int_{\theta_j=0}^{\pi} [q^j(\theta_j, \phi_j) \sin \theta_j] d\theta_j d\phi_j = 1 .$$ (4)

The two kinds of orientation distribution functions may be expanded in a series of the spherical harmonics as follows:[1-3,7)]

$$p(\xi, \phi, \eta) = \sum_{l=0}^{\infty} \sum_{m=-l}^{l} \sum_{n=-l}^{l} W_{lmn} Z_{lmn}(\xi) e^{-im\phi} e^{-in\eta}$$ (5)

and

$$q^j(\zeta_j, \phi_j) = \sum_{l=0}^{\infty} \sum_{m=-l}^{l} Q_{lm}^j P_l^m(\zeta_j) e^{-im\phi_j}$$ (6)

where $Z_{lmn}(\zeta)$ and $P_l^m(\zeta_j)$ are normalized associated Legendre's polynomials having three and two variables, respectively, W_{lmn} and Q_{lm}^j are the coefficients of the expanded series of the distribution functions, and

$$\xi = \cos \theta$$
$$\zeta_j = \cos \theta_j$$ (7)

The coefficients, W_{lmn} and Q_{lm}^j may be given in turn, by the following equations:

$$W_{lmn} = \frac{1}{4\pi^2} \int_{\eta=0}^{2\pi} \int_{\phi=0}^{2\pi} \int_{\xi=-1}^{1} p(\xi, \phi, \eta) Z_{lmn}(\xi) e^{im\phi} e^{in\eta} d\xi d\phi d\eta$$ (8)

and

$$Q_{lm}^j = \frac{1}{2\pi} \int_{\phi_j=0}^{2\pi} \int_{\zeta_j=-1}^{1} q^j(\zeta_j, \phi_j) P_l^m(\zeta_j) e^{im\phi_j} d\zeta_j d\phi_j$$ (9)

The symmetries of the distribution functions expressed by

$$p(\pm\xi, \pi\pm\phi, n\pi\pm\eta) = p(\pm\xi, \pm\phi, n\pi\pm\eta)$$ (10)*

and

$$q^j(\pm\zeta_j, \pi\pm\phi_j) = q^j(\pm\zeta_j, \pm\phi_j)$$ (11)

i.e., orthogonal biaxial-symmetries, may be expected for most of the industrial products, such as polymer films. In addition, the symmetries of the polynomials expressed by

$$Z_{lmn}(\xi) = Z_{lmn}(\xi)$$
$$Z_{lmn}(\xi) = (-1)^{m+n} Z_{lmn}(\xi)$$
$$Z_{lmn}(\xi) = (-1)^{m+n} Z_{lmn}(\xi)$$ (12)

---

* The symmetry about $n\pi \pm \eta$ is reduced from the symmetry of r_j given by Eq. (11).

and

$$P_l^m(\zeta_j) = (-1)^m P_l^m(\zeta_j) \qquad (13)$$

$$P_l^m(-\zeta_j) = (-1)^{l+m} P_l^m(\zeta_j) \qquad (14)$$

are also expected.

These symmetries make the coefficients W_{lmn} and Q_{lm}^j equal to zero when any of l, m or n is an odd number, and not equal to zero only when all of them are even number. Furthermore, the coefficients themselves have the following symmetries:

$$Q_{lm}^j = Q_{l\bar{m}}^l \qquad (15)$$

and

$$W_{lmn} = W_{l\bar{m}\bar{n}} = W_{lm\bar{n}} = W_{l\bar{m}n} \qquad (16)$$

Consequently, the distribution function may be represented by the expanded series only for the even numbers of l, m and n as:

$$p(\xi, \phi, \eta) = \sum_{l=0}^{\infty} W_{l00} Z_{l00}(\xi)$$
$$+ 2 \sum_{l=2}^{\infty} \sum_{m=2}^{l} Z_{lm0}(\xi)\{W_{lm0} \cdot \cos m\phi + W_{l0m} \cos m\eta\}$$
$$+ 2 \sum_{l=2}^{\infty} \sum_{m=2}^{l} \sum_{n=2}^{l} W_{lmn}\{Z_{lmn}(\xi) + Z_{l\bar{m}n}(\xi)\} \cos m\phi \cos n\eta \qquad (17)$$

and

$$q^j(\zeta_j, \phi_j) = \sum_{l=0}^{\infty} Q_{l0}^j P_l(\zeta_j)$$
$$+ 2 \sum_{l=2}^{\infty} \sum_{m=2}^{l} Q_{lm}^j P_l^m(\zeta_j) \cos m\phi_j \qquad (18)$$

A generalization of the Legendre addition theorem gives the following relation:

$$P_l^m(\zeta_j) e^{im\phi_j} = \left(\frac{2}{2l+1}\right)^{1/2} \sum_{n=-l}^{l} Z_{lmn}(\xi) e^{im\Phi} e^{in\eta} P_l^n(\cos \Theta_j) e^{in\Phi_j}, \qquad (19)$$

from which the relationship between W_{lmn} and Q_{lm}^j may be given by

$$Q_{lm}^j = (2\pi)\left(\frac{2}{2l+1}\right)^{1/2}\{W_{lm0} P_l(\cos \Theta_j) + 2\sum_{n=2}^{l} W_{lmn} P_l^n(\cos \Theta_j) \cos n\Phi_j\} \qquad (20)$$

Therefore, in order to determine W_{lmn} from Q_{lm}^j for $l=2l'$, it is necessary to obtain Q_{lm}^j under vanying j from unity to l' plus unity.**

The above discussion proceeded under the orthogonal biaxial-symmetry of the distribution functions as given by Eqs. (10) and (11). On the other hand,

---

** This relation may be useful for determining the degree of orientation of particular crystal plame from those of other crystal planes,[3] as suggested by Sack[8] and Wilchinsky.[9]

Eqs. (17) and (18) may be reduced for the uniaxial-symmetry of the distribution functions by taking every term of $m \neq 0$ in the equations as zero:

$$p(\xi, \eta) = \sum_{l=0}^{\infty} W_{l00} Z_{l00}(\xi) + 2 \sum_{l=2}^{\infty} \sum_{n=2}^{l} W_{l0n} Z_{l0n}(\xi) \cos n\eta \qquad (17')$$

and

$$q^j(\zeta_j) = \sum_{l=0}^{\infty} Q_{l0}^j P_l(\zeta_j) \qquad (18)$$

The orientation factors defined by several different authors, may be understood, in general, in terms of the coefficients of the expanded series W_{lmn} and Q_{lm}^j or the Legendre's polynomials as follows:

$$F_{lmn} = \sqrt{\frac{2}{2l+1} \cdot \frac{(l+m)!}{(l-m)!} \cdot \frac{(l+n)!}{(l-n)!}} \cdot 4\pi^2 W_{lmn}$$

$$= \sqrt{\frac{2}{2l+1} \cdot \frac{(l+m)!}{(l-m)!} \cdot \frac{(l+n)!}{(l-n)!}} \langle Z_{lmn}(\xi) \cos m\phi \cos n\eta \rangle \qquad (21)$$

$$F_{lm0} = \sqrt{\frac{2}{2l+1} \cdot \frac{(l+m)!}{(l-m)!}} \cdot 4\pi^2 W_{lm0}$$

$$= \sqrt{\frac{2}{2l+1} \cdot \frac{(l+m)!}{(l-m)!}} \langle Z_{lm0}(\xi) \cos m\phi \rangle \qquad (22)$$

$$F_{l00} = \sqrt{\frac{2}{2l+1}} \cdot 4\pi^2 W_{l00}$$

$$= \sqrt{\frac{2}{2l+1}} \cdot \langle Z_{l00}(\xi) \rangle \qquad (23)$$

$$F_{lm}^j = \sqrt{\frac{2}{2l+1} \cdot \frac{(l+m)!}{(l-m)!}} 2\pi Q_{lm}^j$$

$$= \sqrt{\frac{2}{2l+1} \cdot \frac{(l+m)!}{(l-m)!}} \langle P_l^m(\zeta_j) \cos m\phi_j \rangle \qquad (24)$$

$$F_{l0}^j = \sqrt{\frac{2}{2l+1}} \cdot 2\pi Q_{l0}^j$$

$$= \sqrt{\frac{2}{2l+1}} \langle P_l(\zeta_j) \rangle \qquad (25)$$

Actually, for examples, F_{200} and F_{20}^j are orientation factors defined by Hermans [4] and Stein [5] for a uniaxial-symmetric system, respectively, F_{220} and F_{22}^j are those defined by Nomura et al. [7] for orthogonally biaxial-symmetric system, and F_{400} and F_{40}^j are defined by Kimura et al. [10] for orthogonally biaxial- or uniaxial-symmetric system. These orientation factors may be given in more concrete forms as follows:

$$F_{200} = \sqrt{\frac{2}{5}} 4\pi^2 W_{200} = \frac{1}{2} (3\langle\cos^2\theta\rangle - 1) \tag{26}$$

$$F_{20}^j = \sqrt{\frac{2}{5}} \cdot 2\pi Q_{20}^j = \frac{1}{2} (3\langle\cos^2\theta_j\rangle - 1) \tag{27}$$

$$F_{220} = \frac{12}{\sqrt{15}} 4\pi^2 W_{220} = 3\langle\sin^2\theta \cdot \cos 2\phi\rangle \tag{28}$$

$$F_{22}^j = \frac{12}{\sqrt{15}} 2\pi Q_{22}^j = 3\langle\sin^2\theta_j \cdot \cos 2\phi_j\rangle \tag{29}$$

$$F_{400} = \frac{\sqrt{2}}{3} 4\pi^2 W_{400} = \frac{1}{8} (35\langle\cos^4\theta\rangle - 30\langle\cos^2\theta\rangle + 3) \tag{30}$$

$$F_{40}^j = \frac{\sqrt{2}}{3} 2\pi Q_{40}^j = \frac{1}{8} (35\langle\cos^4\theta_j\rangle - 30\langle\cos^2\theta_j\rangle + 3) \tag{31}$$

Estimation of Orientation Distribution Function from Orientation Factors

As is will-known, the orientation distribution functions for structural units can not necessarily be determined from experimental sources, except for those of the crystalline units from x-ray diffraction measurements. Usually, the orientations of structural units are obtained as several kinds of averages, i.e., the second or fourth moments of the orientation distributions and further the orientation factors, from optical measurements, such as birefringence and dichroic ratios, as will be discussed later.

Therefore, the estimation of the orientation distribution function $q^j(\theta_j, \phi_j)$ from the coefficients of the expanded series in the spherical harmonics, i.e., the quantities related to the measurable orientation factors through Eqs. (21) to (25), and the error of the estimation against the real distribution function, must be discussed quantitatively. The discussion will be mainly limited to the uniaxial-symmetric system for simplifying the description, however it can be easily extended to the orthogoally biaxial-symmetric system.

Let us substitute the following relations given by

$$f(\zeta_j) = \zeta_j^r \{q^j(\zeta_j)\}^{1/2}$$

and

$$g(\zeta_j) = \zeta_j^s \{q^j(\zeta_j)\}^{1/2}$$

into the following Schwarz inequality

$$\left\{ \int_{-1}^{1} f(\zeta_j) g(\zeta_j) d\zeta_j \right\}^2 \leqq \int_{-1}^{1} \{f(\zeta_j)\}^2 d\zeta_j \int_{-1}^{1} \{g(\zeta_j)\}^2 d\zeta_j, \tag{32}$$

then the relationship between the moments of orientation distribution will be in general given by[3]

$$(\langle \cos^{r+s} \theta_j \rangle)^2 \leqq \langle \cos^{2r} \theta_j \rangle \langle \cos^{2s} \theta_j \rangle . \tag{33}$$

When taking either $r=2l$ and $s=0$ or $r=2l+1$ and $s=1$, then Eq. (33) results in

$$(\langle \cos^{2l} \theta_j \rangle)^2 \leqq \langle \cos^{4l} \theta_j \rangle \tag{34}$$

or

$$(\langle \cos^{2l+2} \theta_j \rangle)^2 / \langle \cos^2 \theta_j \rangle \leqq \langle \cos^{4l+2} \theta_j \rangle \tag{35}$$

In addition, $|\cos \theta_j| \leqq 1$, which means $\cos^{2l} \theta_j \geqq \cos^{2l+2} \theta_j$, then

$$\langle \cos^{2l+2} \theta_j \rangle \leqq \langle \cos^{2l} \theta_j \rangle \tag{36}$$

Fig. 4 illustrates the relationship between the second and fourth moments, i.e., $\langle \cos^2 \theta_j \rangle$ vs. $\langle \cos^4 \theta_j \rangle$, in which the relation should be located within the hatched area irrespective of the type of the distribution function. For example, when the distribution function is given by a Dirac delta function; i.e.,

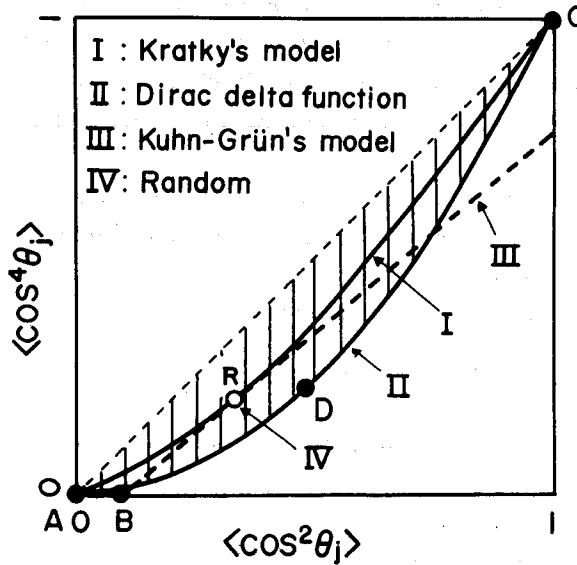$$q^j(\cos \theta_j) = \delta(\theta_j - \theta_{j0}) , \tag{37}$$

Fig. 4. Relationship between the second and fourth moments of several kinds of orientation distribution functions, I: Kratky's floating rod model (First boarderline case), II: Dirac delta function, III: Kuhn and Grün's freely jointed equivalent chain model, IV: random distribution.

the relation is given by the curve ADC; when the distribution is random, the relation is given by the point R; and when the distribution function is given by the Kratky's floating rod model in affine matrix (First boarderline case),[13] the relation is given by the curve ARC. Furthermore, when the distribution function is given by the Kuhn-Grün's freely jointed equaivalent chain model,[14,15] the relation is approximated by a straight line passing through B and R as calculated by Roe[16] postulating Q_{40}^j to be zero.

The coefficient of the expanded series, Q_{lm}^j is generaly given, as already represented by Eq. (24), by a linear combination of the moments of the distribution function. $Q_{2l',0}^j$ is, for example, given by

$$Q_{2l',0}^j = \frac{1}{2\pi} \sqrt{\frac{4l'+1}{2}} \cdot \frac{1}{2^{l'}}$$

$$\sum_{k=1}^{l'+1} \left[(-1)^{l'-k+1} \frac{\prod\limits_{i=1}^{l'}(2k+2i+3)}{(l'-k+1)!(k-1)!} \langle \cos^{2k-2}\theta_j \rangle \right], \tag{38}$$

and Q_{lm}^j may be said to be an orientation factor of the (l, m)th order.

The moments of the orientation distribution function, from which the orientation factors and the coefficients of the expanded series can be calculated as discussed above, could be obtained from several kinds of optically measurable quantities. In general, the dichroic measurements of absorption coefficients or refractive indecis, such as infrared and dye dichromisms or birefringence measurements, give the second moments,[7] and the emission dichroism of polarized fluorescence gives the fourth moments.[10-12]

The relation between the measurable quantities and the moments as well as the orientation factors or the coefficients of the expanded series, can be represented by the following equations:
For the absorption dichroisms or birefringence,[7]

$$\frac{A_3-(A_1+A_2)/2}{A_1+A_2+A_3} = C\frac{3\langle\cos^2\theta\rangle-1}{2}$$

$$= C F_{200} = C 4\pi^2(2/5)^{1/2} W_{200} \tag{39}$$

$$= C'F_{20}^j = C'2\pi(2/5)^{1/2} Q_{20}^j \tag{39}$$

$$\frac{A_1-A_2}{A_1+A_2+A_3} = C\langle\sin^2\theta \cos 2\phi\rangle$$

$$= C F_{220}/3 = C 4\pi^2(16/15)^{1/2} W_{220}/3 \tag{40}$$

$$= C'F_{22}^j/3 = C'2\pi(16/15)^{1/2} Q_{22}^j/3 \tag{40}$$

where A_1, A_2 and A_3 are the absorption coefficients or the refractive indecies for the

polarized radiations along the x_1, x_2 and x_3 axis of the bulk polymer, respectively. The constants, C and C' in the above equations are given by

$$C = (a_{//}^0 - a_\perp^0)/(a_{//}^0 + 2a_\perp^0) \tag{41}$$

and

$$C' = (a_{//}^j - a_\perp^j)/(a_{//}^j + 2a_\perp^j) \tag{42}$$

where $a_{//}^0$ and $a_\perp^0$ are the intrinsic optical constants of the structural unit parallel and perpendicular to the u_3 axis, respectively; $a_{//}^j$ and $a_\perp^j$ are those of the dichroic unit also parallel and perpendicular to the r_j axis, respectively; the dichroic unit is assumed to be adsorbed by the structural unit in accordance with a definite geometric relation; and both units are further assumed to be optically rotational-anisotropic around the u_3 and r_j axis, respectively.

For the fluorescence dichroism, the measurable components of the polarized fluorescence matrix L_{kl} may be given by the following equation:[10]

$$\begin{aligned}
L_{kl} = \;&\{1 - (3/2)\,p\}\{1 - (3/2)\,q\} \langle \cos^2\theta_{kj} \cos^2\theta_{lj} \rangle \\
&+ \{1 - (3/2)\,p\}(q/2) \langle \cos^2\theta_{kj} \rangle \\
&+ \{1 - (3/2)\,q\}(q/2) \langle \cos^2\theta_{lj} \rangle + pq/4
\end{aligned} \tag{43}$$

where the subscripts k and l mean the polarizer and analyzer axes to be parallel to the x_k and x_l axis of the bulk specimen, θ_{kj} or θ_{lj} is the angle between the x_k or x_l axis and the r_j axis of the fluorescent, and p and q are the intrinsic optical constants of the fluorescent for the absorption and emission processes and are given by

$$p = 2a_{//}^j/(a_{//}^j + 2a_\perp^j) \tag{44}$$

and

$$q = 2e_{//}^j/(e_{//}^j + 2e_\perp^j) \tag{45}$$

where the fluorescent is again assumed to be optically rotational-anisotropic body around the r_j axis and to be adsorbed by the structural unit according to a definite geometric relation.

From the above matrix L_{kl}, the new matrix I_{kl} ($\equiv \langle \cos^2\theta_{kj} \cos^2\theta_{lj} \rangle$) may be obtained. From I_{kl}, the following relations to give the second and fourth orientation factors can be reduced:[10]

$$2\pi\sqrt{\frac{2}{5}}\,Q_{20}^j = F_{20}^j = (3\sum_{i=1}^{3} I_{i3} - 1)/2 = (3\sum_{i=1}^{3} I_{3i} - 1)/2 \tag{46}$$

$$2\pi\sqrt{\frac{16}{15}}\,Q_{22}^j = F_{22}^j/3 = \sum_{i=1}^{3}(I_{i1} - I_{i2}) = \sum_{i=1}^{3}(I_{1i} - I_{2i}) \tag{47}$$

$$2\pi\frac{\sqrt{2}}{3}\,Q_{40}^j = F_{40}^j = \frac{1}{8}(35 I_{33} - 30\sum_{i=1}^{3} I_{i3} + 3) \tag{48}$$

$$2\pi\sqrt{5}\,Q^j_{42} = F^j_{42} = \frac{15}{2}\{7(I_{31}-I_{32})-\sum_{i=1}^{3}(I_{1i}-I_{2i})\} \tag{49}$$

$$2\pi\,16\sqrt{35}Q^j_{44} = F^j_{44} = 105(I_{11}+I_{22}-6I_{12}) \tag{50}$$

When one further assumes that the orientation distribution of the structural unit is random around the u_3 axis, i.e., random distribution of angle η, then the following relations can be reduced to:

$$F^j_{2m} = \{(3\cos^2\Theta_j-1)/2\}F_{2m0} \qquad (m=0,\,2) \tag{51}$$

$$F^j_{4m} = (1/8)(35\cos^4\Theta_j-30\cos^2\Theta_j+3)F_{4m0} \qquad (m=0,\,2,\,4) \tag{52}$$

At the present time, there has not been any experimental technique to obtain the higher moments of orientation distribution than the fourth moments, and it would be worthwhile to discuss the error between the real distribution function and the function estimated, as in the above, from the moments.

The average square error may be given by[1-3]

$$\sigma^2_q = \int_{-1}^{1}\{q^j(\zeta_j)-\sum_{l=0}^{l_1}Q^j_{2l}P_{2l}(\zeta_j)\}^2 d\zeta_j \tag{53}$$

From the orthogonality of the Legendre polynomials $P_{2l}(\zeta_j)$, Eq. (53) may be reduced to:

$$\sigma^2_q = \int_{-1}^{1}\{q^j(\zeta_j)^2\}d\zeta_j-\sum_{l=0}^{l_1}(Q^j_{2l})^2 \tag{54}$$

or

$$\sigma^2_q = \sum_{l=l_1+1}^{\infty}(Q^j_{2l})^2 \tag{55}$$

For random orientation, $q^j(\zeta_j)=0.5$, and $Q^j_{2l}=1$ or 0 for $l=0$ or not zero. This means that the average square error, σ^2_q is zero even when l_1 is taken as small zero. On the other hand, the sharper the distribution function, the larger the value within the integration in the righthand side of Eq. (54) and the error itself. This means that the sharper the orientation distribution, the higher order of l_1 should be taken into account for approaching the real distribution.

Let us evaluate the error quantitatively by using a uniaxial-symmetric orientation distribution function proposed by Kratky as a floating rod model in the affine matrix:[13] i.e.,

$$p(\theta,\,\phi)\sin\theta\,d\theta\,d\phi = \frac{1}{4\pi}\frac{\lambda^3}{\{\lambda^3-(\lambda^3-1)\cos^2\theta\}^{3/2}}\sin\theta\,d\theta\,d\phi \tag{56}$$

where λ is the stretch ratio of the bulk specimen along the symmetric axis.
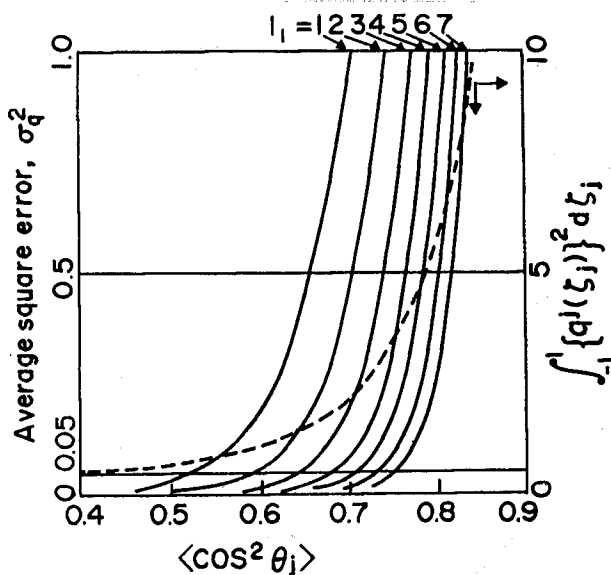
Fig. 5. Changes of the intergrated value $\int_{-1}^{1} \{q^j(\zeta_j)\}^2 d\zeta_j$ and the average square error $\sigma_q{}^2$ under varying l_1 from 1 to 7, both with the increase of $\langle \cos^2 \theta_j \rangle$.

Fig. 5 shows the changes of $\int_{-1}^{1} \{q^j(\zeta_j)\}^2 d\zeta_j$ and the error both with the increase of $\langle \cos^2 \theta_j \rangle$ being accompanied with the increase of λ. In order to keep the error less than 5%, it may be enough to take l_1 as unity, i.e., to take the second moment alone into account unless $\langle \cos^2 \theta_j \rangle$ is larger than 0.5; however, it is necessary to take l_1 to be larger than unity, i.e., to take the fourth and sixth moments as well into account unless $\langle \cos^2 \theta_j \rangle$ is larger than 0.6; and so on.[3]

Fig. 6 shows a comparison of the Kratky's distribution function at various stretch ratios around 2, which is indicated by a solid line, with the distribution function calculated from the summation of the moments while keeping the error in a range as small as from 2% to 3.5%.[3] It may be seen again that the larger the stretch ratio, i.e., the larger the value of $\langle \cos^2 \theta_j \rangle$, the higher the moments should be considered in order to approach the real distribution function.

Orientation Behavior of Crystalline Polymers during Mechanical Drawing

In this section, two types of characteristic orientation behavior of semicrystalline polymers during uniaxially stretching, will be demonstrated in terms of the orienta-
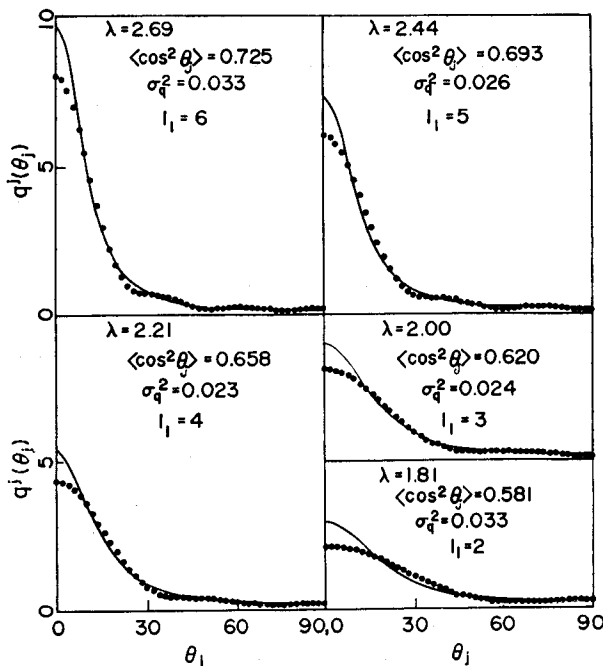
Fig. 6. Comparison of the Kratky's distribution function at
various stretch ratios around 2 with the distribution
functions calculated from the summation of the
moments while keeping the error in a range from
2 to 3.5%.

tion factors of cyrstalline and noncrystalline phases on the basis of the biphase
structure.

Orientation Behavior of Polyvinyl Alcohols during Uniaxially Stretching and after Releasing at Relatively High Humidity

Fig. 7 shows the orientation behavior of crystalline phase of three types of
polyvinyl alcohols, atactic, syndiotactic, and isotactic polymers, at relatively
high humidity around 80% r.h. at 20°C.[17] As recognized from the figure, the
orientation behavior of the crystal b axis (molecular direction) in terms of the
orientation factor F_{20}^j shows positive orientation, while that of the crystal a^* and
c axis shows negative orientation.   In details, it may be noted that the negative
orientations of the crystal a^* and c axis, which are taken as perpendicular to the
b axis and are orthogonal to each other, are quite similar, and that the behavior
during stretching coincides to the behavior after releasing for every crystal axis.   In
other words, the orientation behavior of the crystalline phase may be represented by
the preferential positive orientation of the crystal b axis, around which the crystallites
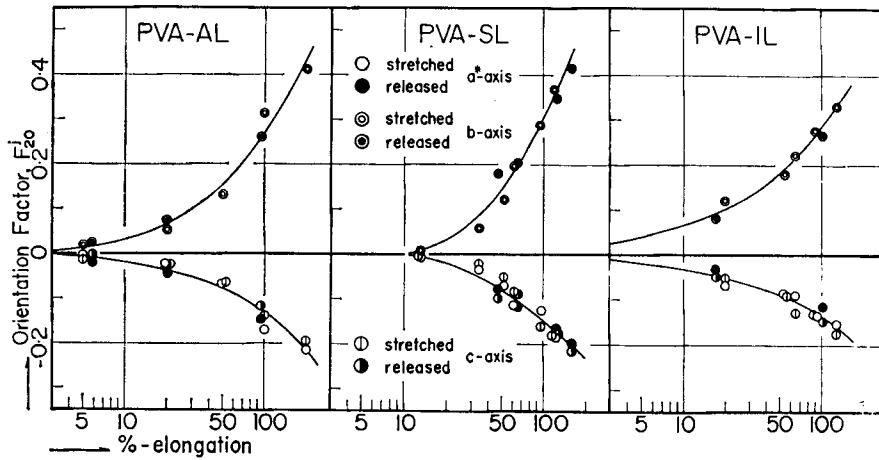
Fig. 7. Orentation behavior of crystalline phases of three types of polyvinyl alcohols in terms of the change of orientation factor F_{20}^j of the jth crystallographic axis (a^*, b, and c axes), with %-elongation during uniaxially stretching or residual %-elongation after releasing at around 80% r.h. at 20°C.

orient randomly so that the orientation distribution function of the crystallites, $p(\theta, \phi, \eta)$ can be given by the random distributions of angles ϕ and η.

These facts suggest the validity of the Kratky's floating rod model as the morphological model for the polyvinyl alcohols; i.e., the crystallites float freely within swollen noncrystalline matrix with almost non-interaction between crystallites.

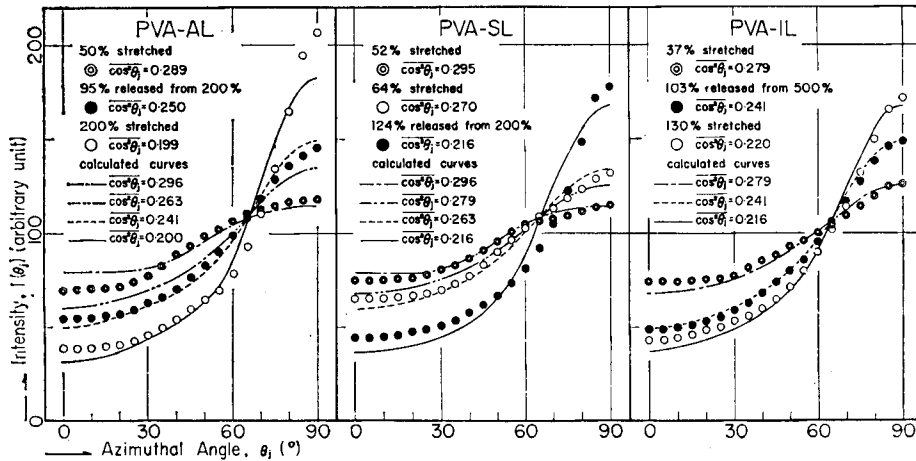Fig. 8 shows comparison of the orientation distribution functions of paratropic

Fig. 8. Comparison of the orientation distributions of paratropic planes of polyvinyl alcohol crystal (101)/(101) observed from x-ray diffraction, with those calculated from the Kratky's model so that the second moment of orientation distribution function $\langle \cos^2 \theta_j \rangle$ calculated from the model agrees with that observed.

planes $(101)/(10\bar{1})$ observed from x-ray diffraction, with those calculated from the Kratky's model so that the second moment of distribution function, $\langle\cos^2\theta_j\rangle$ calculated from the model agrees with that observed. There are fairly good agreements between the calculated and observed distribution functions except for the functions of atactic and syndiotactic polymers at relatively high-elongations.

Fig. 9 shows the orientation behavior of noncrystalline phase of the three types of polyvinyl alcohols[17]. The orientation behavior of noncrystalline chain segments
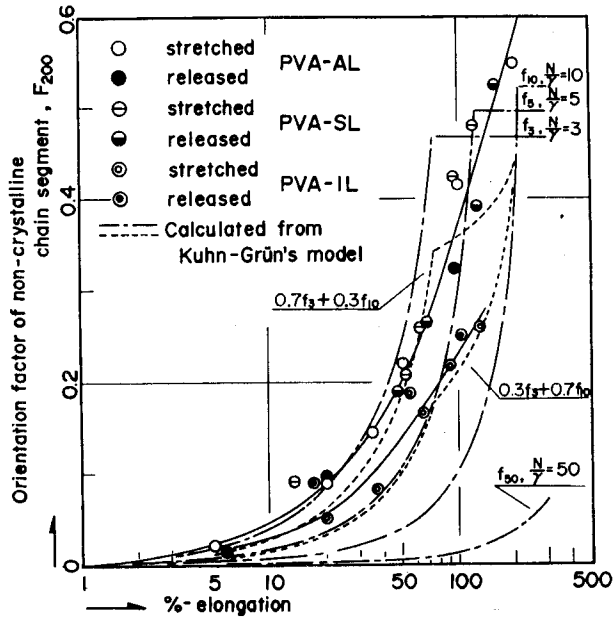

Fig. 9. Comparison of orientation behavior of noncrystalline phases of three types of polyvinyl alcohols with that predicted from fractional contributions of the Kuhn and Grün's freely jointed equivalent chain model by varying the value of N/γ from 3 to 10.

in terms of the orientation factor F_{200} seems to be represented by fractional contribution of the Kuhn-Grün's freely jointed equivalent chain model[14] varying the value of N/γ in a range of as small as from 3 to 10, where N is the number of statistical segments and γ is the ratio of mean square end-to-end distance of the actual chain to that of the Gaussian chain in the undeformed state. In other words, the noncrystalline chains are expected to elongate considerably even in the undeformed state.

As a result, it may be concluded that the orientation behavior of the crystalline and noncrystalline phases of the polyvinyl alcohols during uniaxially stretching at

relatively high humidity, can be represented by the Kratky's floating rod model and the Kuhn-Grün's freely jointed equivalent chain model, respectively; i.e., the behavior can be represented by a relatively simple affine deformation of the noncrystalline matrix, in which the crystallites float with almost non-interaction between each other.

This may consist with the morphology of the polyvinyl alcohols lacking any super-structure of crystal aggregation, although the crystal structure is still uncertain whether it is characterized by the classical fringed miceller type or the folded chain type.

Orientation Behavior of Poly-alpha-olefines during Uniatially Stretching

In contrast to the above behavior, the orientation behavior of two types of of poly-alpha-olefines, polyethylene and isotactic polypropylene, during uniaxially stretching will be demonstrated. These polymers, when cast from molten state, have more or less crystalline super-structure, so-called the spherulite structure, irrespective of their annealing conditions.

Fig. 10 shows the orientation behavior of crystalline phase of two types of polyethylene, low and high density polyethylenes, in terms of the orientation factors F_{20}^j of the three principal crystal axes of the crystallite during uniaxially stretching at a room temperature around 20°C.[18] As seen in the figure, the crystal c axis (molecular chain direction) shows positive orientation, while the crystal a and b
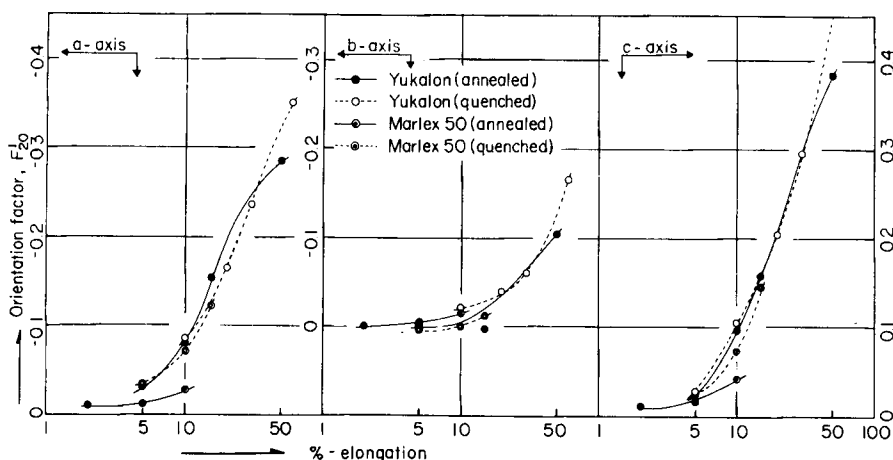

Fig. 10.   Orientation behavior of crystalline phases of two types of polyethylenes, low and high density polyethylenes, in terms of the change of orientation factor F_{20}^j of the jth crystallographic axis (a, b, and c axes) with %-elongation during uniaxially stretching at 20°C.

axes, which are perpendicular to the crystal c axis and are in orthogonal relation
to each other, show negative orientation.   In detail, however, predominant negative
orientation of the crystal a axis over the b axis can be seen, which is in contrast to
the equally negative orientagion of the crystal a^* and c axis of the polyvinyl alcohols.
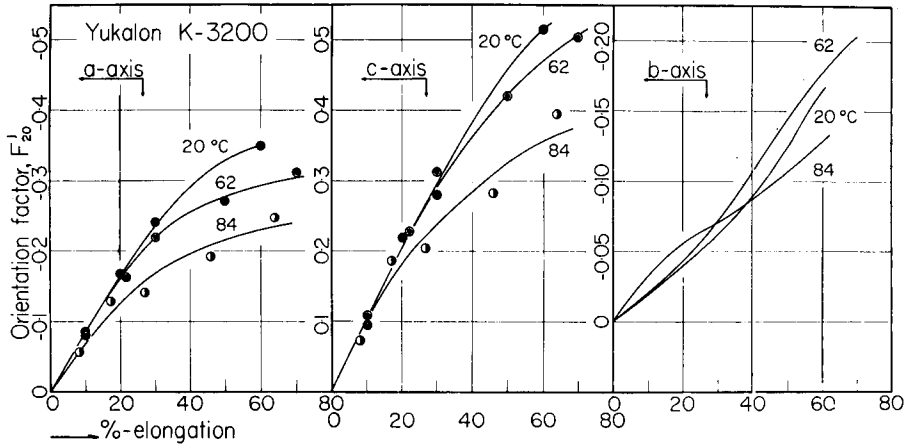

Fig. 11.   Change of orientation behavior of polyethylene crystals with increasing of stretch-
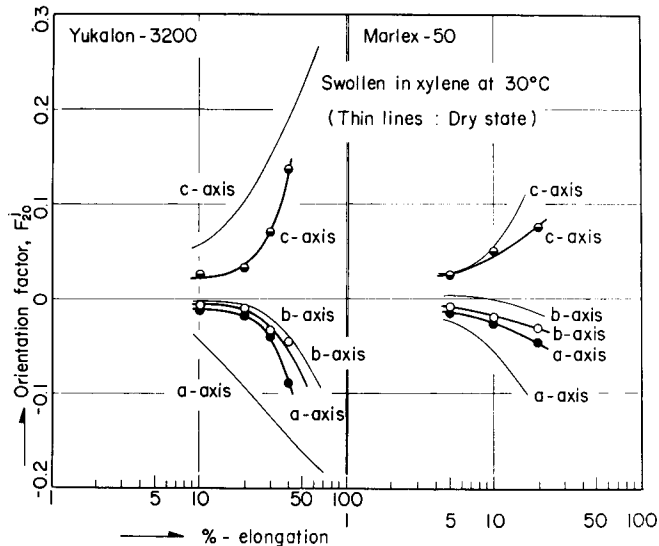ing temperature upto near the crystal disordering temperature for a low density
polyethylene.

Fig. 12.   Orentation behavior of crystalline phases of two types of
polyethylenes, low and high density polyethylenes, in
terms of the change of orientation factor F_{20}^j of the jth
crystallographic axis $(a, b, $ and c axes) with %-elongation
during uniaxially stretching in xylene at 30°C,

Fig. 11 and 12 show the orientation behavior of the crystalline phase of a low density polyethylene at elevated temperatures near crystal disordering temperature [19] and that of two types of polyethylenes, low and high density polyethylenes, at a swollen state in xylene at 30°C.[20]　It may be seen in the figures that the predominant negative orientation of the crystal *a* axis diminishes and approaches to the equally negative orientation with the elevation of the stretching temperature or the swelling in xylene.

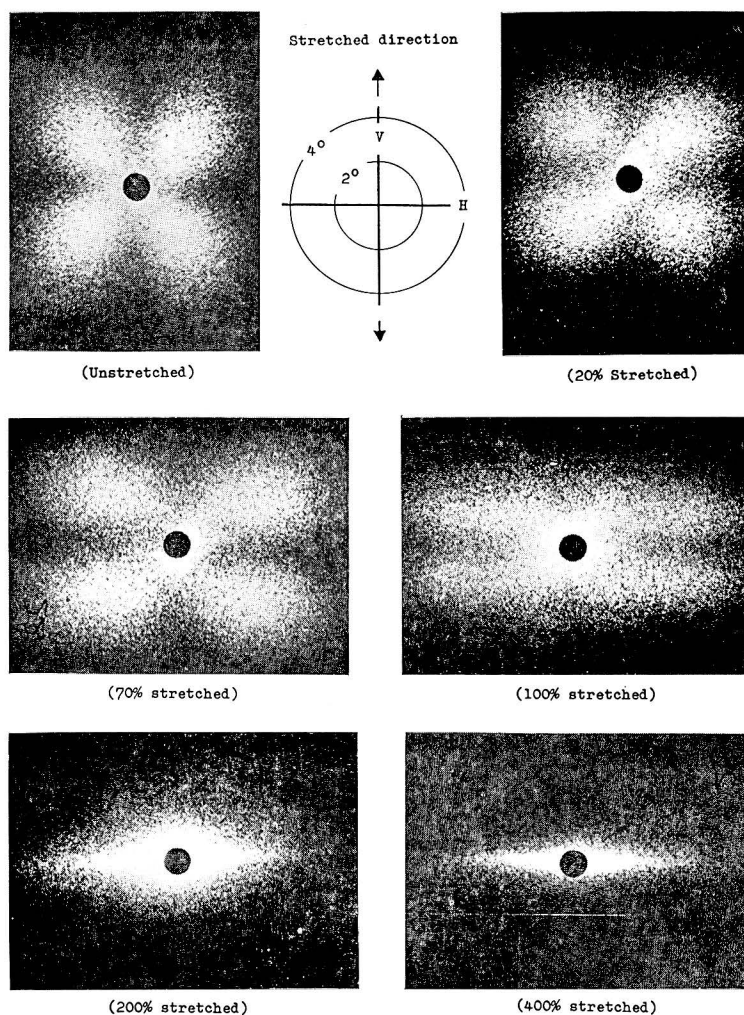This may be interpreted in such ways that the orientation behavior must be,

Fig. 13.　Change of small angle H_v light-scattering pattern from isotactic polypropylene film (molten cast and annealed at 160°C.) with uniaxially stretching up to 400 %-elongation at 130°C.

at first, governed by the deformation mechanism of the crystal super-structure, a regular aggregation of the crystallites so as to form the spherulite, and that the elevation of the stretching temperature or the swelling in xylene makes the intraction between the crystallites so weak as to disintegrate the super-structure during stretching and individualizes the orientation behavior as that of the crystallite itself.

As an experimental justification for the above discussion, Fig. 13 shows the change of small angle H_v light-scattering pattern from isotactic polypropylene film, [21] which was molten-cast, annealed at 160°C., and stretched uniaxially by various %-elongations at 135°C. The scattering patterns are well-known "four leaf clover pattern" at unstretched state and its modifications at stretched states upto a critical %-elongation around 200%, respectively, which are well-correlated with the deformation of the spherulite.[22-25] However, when the %-elongation exceeds the critical value, the pattern chages from the four leaves to two streaks along the H and V directions. This suggests a disintegration of the regular spherulite structure at the critical %-elongation.

The orientation behavior of crystalline phase of the polypropylene during the uniaxially stretching is illustrated in Fig. 14 in terms of the orientation factors of three orthogonal axes of the polypropylene monoclinic crystal F_{20}^j, where the crystal c axis is taken as being parallel to the molecular direction and the crystal a^* and b axes are taken as being perpendicular to the molecular direction and orthogonal to each other. As seen in the figure, the crystal c axis shows positive orientation, while the crystal b axis, instead of the a axis in the case of polyethylene, shows the predominant negative orientation over the a^* axis until the degree of stretching attains the critical %-elongation, beyond which the equally negative orientations of the a^* and b axes appear[21].
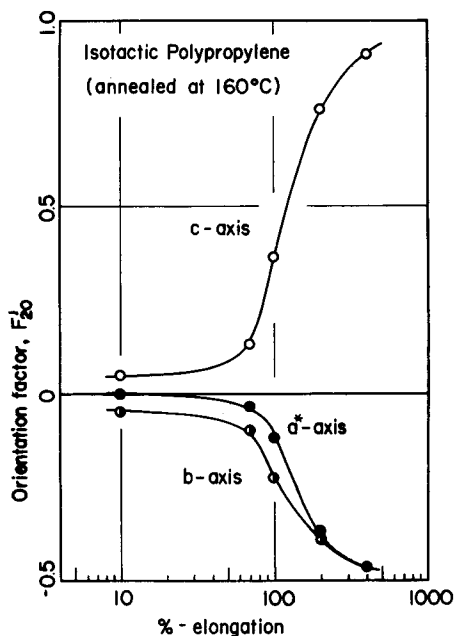

Fig. 14. Orientation behavior of crystalline phase of isotactic polypropylene (molten-cast and annealed at 160°C.) in terms of the change of orientation factor F_{20}^j of the jth crytallographic axis (a^*, b, and c axes.) with %-elongation during uniaxially stretching at 130°C.

   The deformation mechanism of poly-alpha olefine spherulite has been studied by many authors.[17,18,26-36]   Among them, quantitative description was made by Stein et al. as well as Kawai et al. using essentially the same model, as shown in Fig. 15 for polyethylene spherulite.   In the model, the crystal lamella is taken as
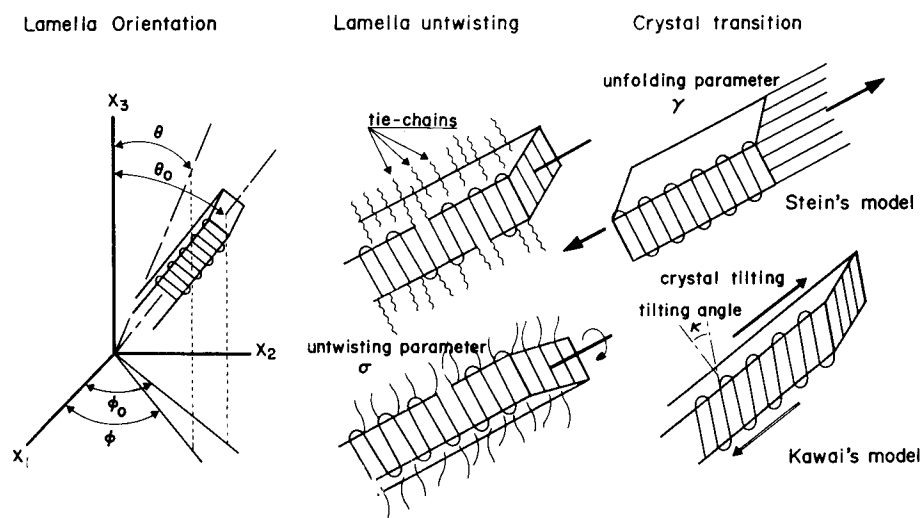

Fig. 15.   Schematic illustrations of deformation mechanism of polyethylene spherulite, upper: Stein's model taking into account the crystal transition and the lamella untwisting, lower: Kawai's model taking into account the crystal tilting and the lamella untwisting.

the orientation unit within the affine matrix, with taking into accound either the crystal transition from the folded chain type to the fiber type crystal due to micro-necking of the lamella along the lamella axis or the crystal tilting toward the 100 direction due to shearing along the lamella surface in combination with the untwisting of lamella around the lamella axis due to straining of the tie chains between the lamellae.

   According to the Kawai's model, the orientation distribution function of the crystal lamellae within the affine matrix, may be given by[37]

$$p_{\text{lamella}}(\theta, \eta) = N(\theta)\{1 + \sigma \cdot g(\theta) \cdot \cos 2\eta\} \tag{57}$$

where $N(\theta)$ is the same distribution function as given by Eq. (56) for the Kratky's floating rod model, σ is a parameter of easiness of the lamella untwisting around the lamella axis, and $g(\theta)$ is a function proposed by Stein as[31]

$$g(\theta) = (\lambda - 1) \sin^2 \theta \tag{58}$$

so that the lamella untwisting is mostly concentrated at the equatorial zone but

slightly at the polar zone of uniaxially deformed spherulite.

The coefficients of the expanded series of the distribution function of the crystal lamella, may be given by

$$2\pi \cdot W_{2l} = \int\limits_0^{2\pi} \int\limits_0^{\pi} Z_{2l,00}(\cos \theta) \; p_{\text{lamella}}(\theta, \eta) \sin \theta \, d\theta \, d\eta \tag{59}$$

$$2\pi \cdot W_{2l,2} = \int\limits_0^{2\pi} \int\limits_0^{\pi} Z_{2l,20}(\cos \theta) \cos 2\eta \; p_{\text{lamella}}(\theta, \eta) \sin \theta \, d\theta \, d\eta \tag{60}$$

and the other $W_{2l,2m}$ is zero.

The distribution function of the jth axis $q^j(\theta_j)$ can be given by

$$q^j(\theta_j) = \sum_{l=0}^{\infty} Q_{2l}^j \cdot P_{2l}(\cos \theta_j) \tag{61}$$

where Q_{2l}^j, the coefficients of the expanded series of the distribution function of the jth axis within the crystal lamella, can be further given from Eq. (20) as follows:

$$Q_{2l}^j = \sqrt{\frac{2}{4l+1}} \{2\pi \, W_{2l} \cdot P_{2l}(\cos \Theta_j) + 2(2\pi \cdot W_{2l,2}) P_{2l}^2(\cos \Theta_j) \cos 2\Phi_j\} \tag{62}$$

The geometric relationship of the three principal crystal axes of polyethylene crystal (orthorhombic), a, b and c axis, and the reciprocal lattice vector of (110) crystal plane within the lamella, is listed in the following table in terms of the angles, Θ_j and Φ_j and the tilting angle κ toward the 100 direction of the original lamella:

	$\cos \Theta_j$	$\cos 2\Phi_j$
a axis	0	-1
b axis	$\cos \kappa$	1
c axis	$-\sin \kappa$	1
$(110)_N$	$\cos \kappa \cdot \cos 33.69°$	$\dfrac{\sin^2 \kappa - \tan^2 33.96°}{\sin^2 \kappa + \tan^2 33.69°}$

Fig. 16 shows comparison of the azimuthal distributions of x-ray diffraction intensity from (110) crystal plane, the most intensive reflection, for a low density polyethylene stretched by 50%–elongation under various envilonmental conditions with the distributions calculated from Eqs. (62) and (63) by varying the untwisting parameter σ and the tilting angle κ for some extent.[37]

Although there exist considerable discrepancies between the calculated and observed results, it may be understood that the tilting angle κ should be taken as being larger than, at least, 60°, and that the effect of the untwisting is rather minor
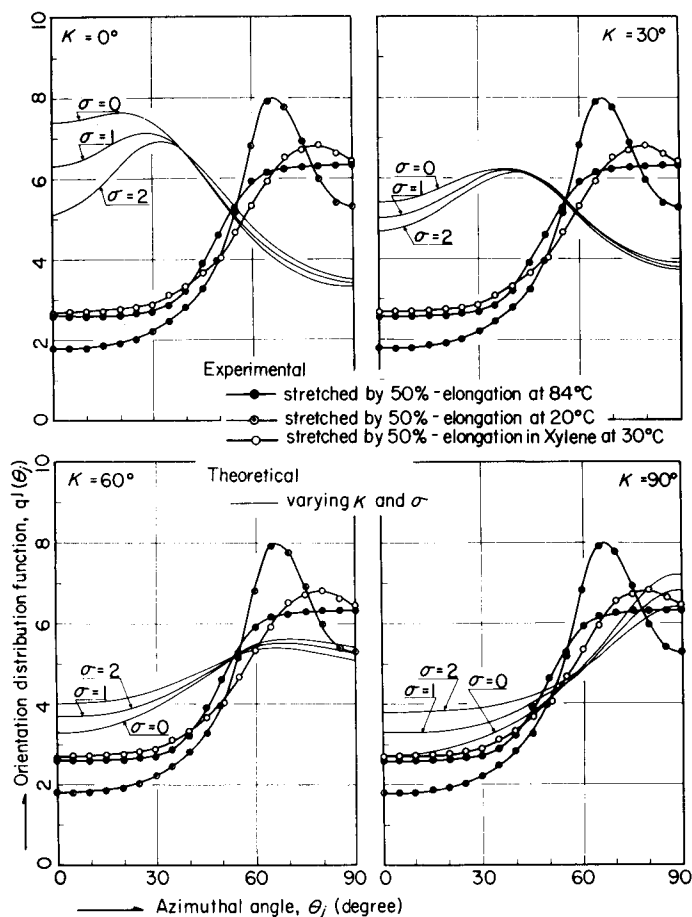
Fig. 16. Comparison of orientation distribution of (110) crystal planes
obseved from x-ray diffraction for a low density polyethylene
stretched uniaxiallly by 50%-elongation under various en-
vilonmental conditions, with those calculated from Eqs. (62)
and (63) by varying the untwisting parameter σ and the
tilting angie κ.

in this model.   The discrepancies may be improved when one takes the tilting angle
κ as a function of lamella orientation angle θ.

Mechanical Anisotropy of Crystalline Polymers in Relation to Molecular Orientations

In this section, the mechanical anisotropy of crystalline polymers in relation
to molecular orientation will be discussed by taking biaxially or uniaxially stretched
polypropylene films as examples of anisotropic systems.

The orientation behavior of crystalline polymers during biaxially stretching

has been rarely published, and, therefore, the behavior during strip-biaxially and orthogonal-biaxially stretching will be first demonstrated, and then the mechanical anisotropy will be discussed in terms of the molecular orientations on the basis of either the homogeneous stress or strain hypothesis.

Orientation Behavior of Isotactic Polypropylene during Orthogonal—Biaxially Stretching

As a typical example, Fig. 17 shows an x-ray diffraction diagram obtained from radiation along the transverse direction of a film specimen of isotactic polypropylene, which was stretched orthogonal-biaxially upto more than 300%-elongation at elevated temperature near 130°C. The diffraction pattern is primarily a type of monoclinic crystal system and seems to consist of three types of orientations, as illustrated schematically in the middle column in the figure by α, β, and γ types.

The α type orientation is characterized by a preferential planar orientation of (040) crystal plane parallel to the film surface. The β type orientation begins to appear subsidarily at around 100%-elongation, and is characterized by a preferential orientation of (110) crystal plane being inclined by about 55° to the film
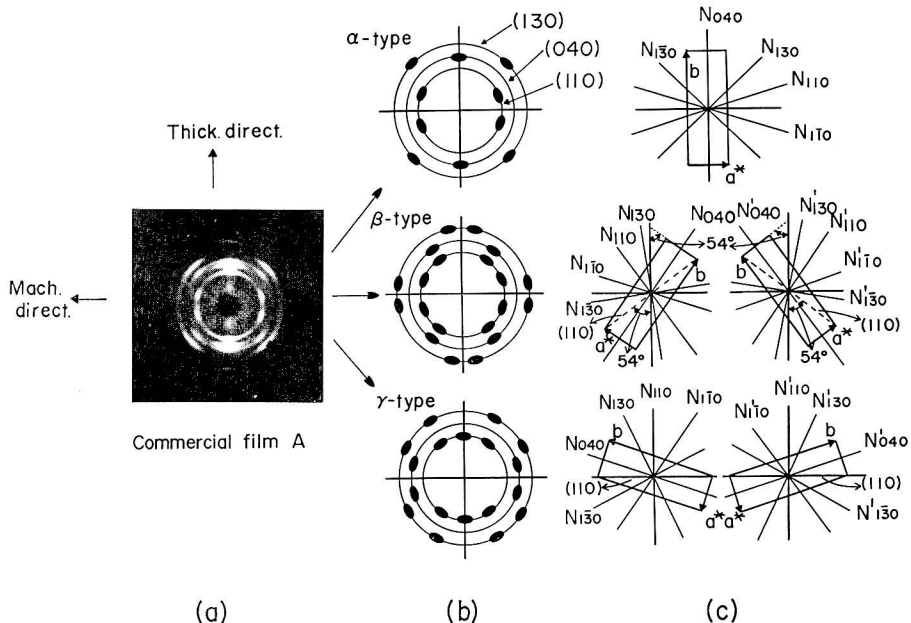

Fig. 17. (a): typical x-ray diffraction diagram obtained from radiation along the transverse direction of highly orthogonal-biaxially stretched polypropylene film (commercial film A), (b): schematic representations of three type diffractions composing the x-ray diagram, (c): schematic representation of crystal orientations corresponding to the three types of diffractions.

normal probably due to (110) twinning of a part of α type oriented crystals.   The γ type orientation appears when releasing the stretched film at relatively high temperature but does not appear when quenching the stretched film under tension, and is characterized by a preferential planar orientation of (110) crystal plane along the film surface probably due to further (110) twinning of a part of β type oriented crystals.[38]

For visual convenience, the biaxial orientation behavior will be demonstrated in terms of the second moment of orentation distribution function of the jth crystal axes with respect to the x_i reference axis in the blulk specimen; i.e., in terms of $\langle \cos^2 \theta_{ji} \rangle$, instead of the biaxial orientation factors, F_{220} or F_{22}^j defined by Eqs. (28) or (29), by using the equilateral triangle coordinate system proposed by Desper.[39]

The orientation behavior of crystal a^*, b and c axes is shown in the first, second and third column in Fig. 18, and that of noncrystalline chain segment in the fourth column, respectively.   The upper row is the result during orthogonal-biaxially stretching, the middle row is the result durning strip-biaxially stretching, i.e., un-
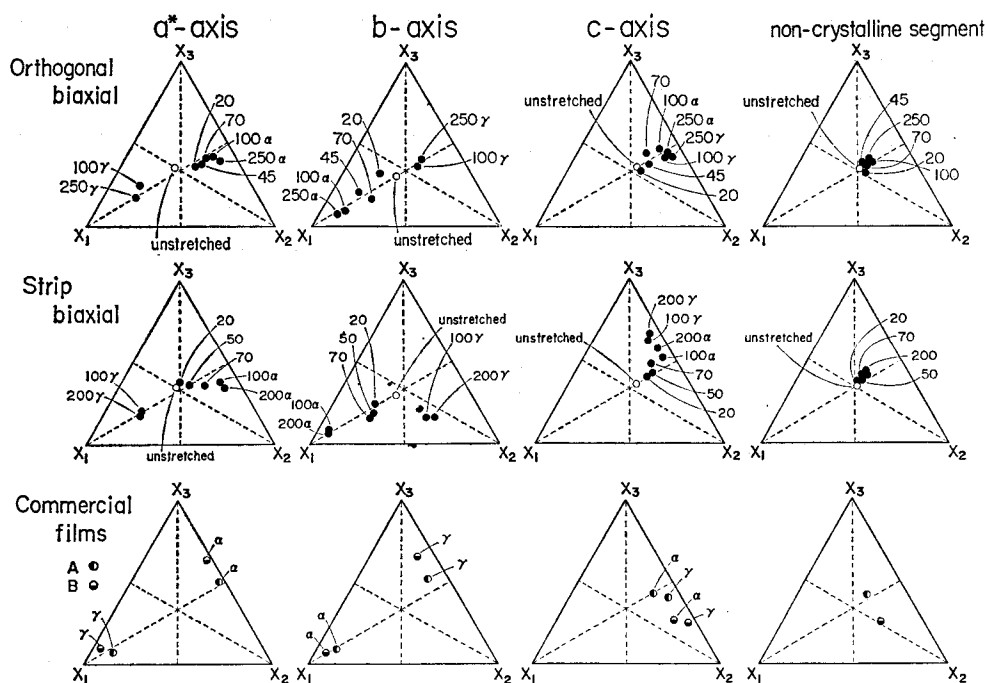

Fig. 18.   Orientation behavior of crystalline and noncrystalline phases of isotactic polypropylene films in terms of the changes of orientation factors F_{20}^j of the crystal a^*, b, and axes and F_{200} of the noncrystalline chain segment, with %-elongation during two types of biaxially stretching at 130°C.   The open circle indicates original film (extruded and unstretched).

iaxially stretching while keeping the width of the specimen along the transverse
direction constant, and the lower row is that for two kinds of commercial films.

As seen in the figure, the α type orientation behavior of crystalline phase during
the orthogonal-biaxially stretching is characterized by the preferential orientation
of the crystal b axis toward the x_1 direction (thickness direction) around which the
crystal a^* and c axes orient at random.   On the other hand, the γ type orientation
is characterized by the preferential orientation of the crystal a^* axis toward the x_1
direction around which the crystal b and c axes orient randomly, where the β type
orientation is not found in this case probably because of almost complete conversion
to the γ type orientation.

During the strip-biaxially stretching, the above orientation behavior is modi-
fied in such ways that the random orientations of the crystal a^* and c axes for the α
type orientation are concentrated toward the x_2 direction (transverse direction) and
the x_3 direction (machine direction), respectively, and that the random orientation
of the crystal b and c axes for the γ type orientation are concentrated toward the
x_2 and x_3 directions, respectively.

The orientation behavior of the noncrystalline chain segment is principally the
same as that of the crystal c axis but to a far less extent.

From the above results, the orientation behavior of the two kinds of com-
mercial films, A and B, may be interpreted in the following ways; i.e., both films
must be extremely highly stretched biaxially; and the degrees of stretching along the
machine and transverse directions are rather balanced for film A, but unbalanced
for film B for which the degree of stretching along the transverse direction must
proceed over that along the machine direction.

Mechanical Anisotropy of Crystalline Polymers in Relation
to Molecular Orientation

The mechanical anisotropy of crystalline polymers in relation to molecular
orientation has been extensively studied by Ward et al.[40-45] using the so-called
"aggregation model" of structural units on the basis of either the homogeneous
stress or the homogeneous strain hypothesis.   The studies by Ward et al. are,
however, concentrated on the uniaxially oriented system of monophase structure,
and, therfore, the discussion may be desirable to extend to orthogonal-biaxially
oriented system of biphase structure, crystalline and noncrystalline phases, based
on the orientation data of polypropylene obtained above.

Fig. 19 shows the angular dependence of tensile dynamic modulus of the com-
mercial films, A and B, measured along various directions within the film plane by
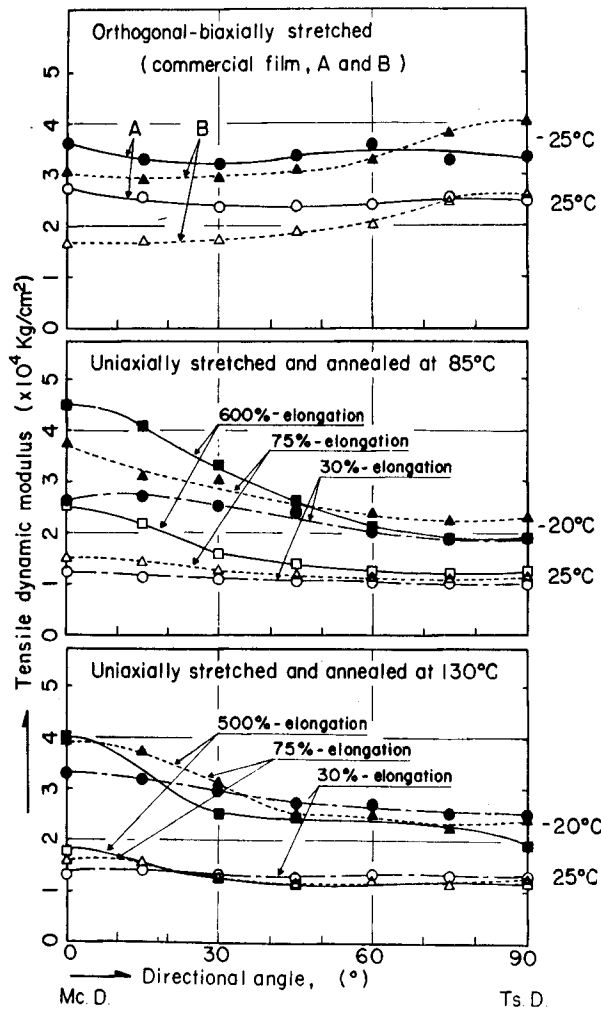
Fig. 19. Mechanical anisotropy of oriented polypropylene films in terms of angular dependence of tensile dynamic modulus measured along various directions within the film plane at a fixed frequency 110 cps at two different temperatures, below and beyond the glass transition temperature of this polymer. Upper: highly orthogonal-biaxially stretched films (commercial fiims, A and B), middle: uniaxially stretched films (quenched from melt, stretched at room temp. and annealed at 85°C. under fixed length), lower: uniaxially stretched films (quenched from melt, stretched at room temp. and annealed at 130°C. under fixed length).

using the Viscoelastic spectrometerr[6] at a fixed frequency 110 cps at two different
temperatures, -25 and $+25°C.$, below and beyond the galss-transition temperature
of this polymer. The data at -20 and $+25°C.$ for two series of uniaxially stretched
specimens (quenched from melt, stretched at room temperature, and annealed under
fixed length at two different temperatures, 85 and 130°C.), are also included in the
middle and lower parts in the figure. As seen in the figure, the angular dependence
of the tesile dynamic modulus is rather minor but definite, and is well correlated,
for examples for the commercial films, with the planar orientations of the crystal
c-axis and the noncrystalline chain segment within the film plane; i.e., the mechani-
cal anisotropy is well balanced for film A, but rather concentrated toward the trans-
verse direction for film B.[47]

On the basis of the homogeneous stress hypothesis,[48] the tensor of the elastic
compliances of the crystalline phase, an aggregate of crystallites, s^c_{ijkl} can be
expressed by

$$s^c_{ijkl} = \langle a_{ip} a_{jq} a_{kr} a_{ls} \rangle_{av} s^{co}_{pqrs} \tag{63}$$

and, silimarily, on the basis of the homogenous strain hypothesis,[49] the tensor of
the eleastic stiffness of the aggregate, c^c_{ijkl} can be expressed by

$$c^c_{ijkl} = \langle a_{ip} a_{jq} a_{kr} a_{ls} \rangle_{av} c^{co}_{pqrs} \tag{64}$$

where a_{ip} is, for example, the direction cosine of the U_p axis of the crystalline
structural unit with respect to the x_i axis of the crystalline phase, s^{co}_{pqrs} and c^{co}_{pqrs}
are the elastic compliances and stiffnesses of the unit, respectively. These expres-
sions for averaging are, of course, two extreme approximations of the real situation
of polycrystalline materials, as frequently pointed out by several authors,[50-52] for
example, by Gupta,[45] Kausch,[53] and Nomura,[54] quite recently.

These expressions may be expanded to polyphase system, such as biphase
system in the simplest case, as follows:

$$s_{ijkl} = X_c s^c_{ijkl} + (1 - X_c) s^a_{ijkl} \tag{65}$$

and

$$c_{ijkl} = X_c c^c_{ijkl} + (1 - X_c) c^a_{ijkl} \tag{66}$$

where X_c is the degree of crystallinity in volume fraction, and s^a_{ijkl} and c^a_{ijkl} are
elastic compliances and stiffnesses of the noncrystalline phase and are described
similarily as in Eqs. (63) and (64) in terms of the compliances and stiffnesses of
the noncrystalline structural unit, s^{ao}_{pqrs} and c^{ao}_{pqrs} respectively.

Compliances and stiffnesses of the crystalline phase, such as s^c_{ij}, c^c_{ij} and c^c_{pp} can
be written in terms of the second and fourth moments of orientation distribution

of the crystalline structural units and its mechanical constants as follows:[54]

$$s_{ii}^c = \langle \sin^4 \theta_{i,3} \rangle s_{11}^{co} + \langle \cos^4 \theta_{i,3} \rangle s_{33}^{co} + \langle \cos^2 \theta_{i,3} \sin^2 \theta_{i,3} \rangle (2s_{13}^{co} + s_{44}^{co}) \tag{67}$$

$$s_{ij}^c = \langle \cos^2 \theta_{i,3} \cos^2 \theta_{j,3} \rangle (s_{11}^{co} + s_{33}^{co} - s_{44}^{co}) + \langle (1 - \cos^2 \theta_{i,3} - \cos^2 \theta_{j,3}) \rangle s_{12}^{co}$$
$$+ \langle (\cos^2 \theta_{i,3} + \cos^2 \theta_{j,3} - 2 \cos^2 \theta_{i,3} \cos^2 \theta_{j,3}) \rangle s_{13}^{co} \tag{68}$$

$$s_{pp}^c = \langle \cos^2 \theta_{i,3} \cos^2 \theta_{j,3} \rangle (4s_{11}^{co} + 4s_{33}^{co} - 8s_{13}^{co} - 4s_{44}^{co})$$
$$+ 2 \langle (1 - \cos^2 \theta_{i,3} - \cos^2 \theta_{j,3}) \rangle (s_{11}^{co} - s_{12}^{co})$$
$$+ \langle (\cos^2 \theta_{i,3} + \cos^2 \theta_{j,3}) \rangle s_{44}^{co} \tag{69}$$

$$c_{ii}^c = \langle \sin^4 \theta_{i,3} \rangle c_{11}^{co} + \langle \cos^4 \theta_{i,3} \rangle c_{33}^{co} + 2 \langle \cos^2 \theta_{i,3} \sin^2 \theta_{i,3} \rangle (c_{13}^{co} + 2c_{44}^{co}) \tag{70}$$

$$c_{ij}^c = \langle \cos^2 \theta_{i,3} \cos^2 \theta_{j,3} \rangle (c_{11}^{co} + c_{33}^{co} - 4c_{44}^{co})$$
$$+ \langle (1 - \cos^2 \theta_{i,3} - \cos^2 \theta_{j,3}) \rangle c_{12}^{co}$$
$$+ \langle (\cos^2 \theta_{i,3} + \cos^2 \theta_{j,3} - 2 \cos^2 \theta_{i,3} \cos^2 \theta_{j,3}) \rangle c_{13}^{co} \tag{71}$$

and

$$c_{pp}^c = \langle \cos^2 \theta_{i,3} \cos^2 \theta_{j,3} \rangle (c_{11}^{co} + c_{33}^{co} - 2c_{13}^{co} - 4c_{44}^{co})$$
$$+ (1/2) \langle (1 - \cos^2 \theta_{i,3} - \cos^2 \theta_{j,3}) \rangle (c_{11}^{co} - c_{12}^{co})$$
$$+ \langle (\cos^2 \theta_{i,3} + \cos^2 \theta_{j,3}) \rangle c_{44}^{co} \tag{72}$$

where the mechanical anisotropy of the structural unit is assumed to be rotational ellipsoid around the U_3 axis, and $i = 1, 2, 3$; $i, j = 1, 2, 3$; and $p = 4, 5, 6$.

The compliances and stiffnesses of the noncrystalline phase may be described similarly to the above in terms of the degree of biaxial orientation of the noncrystalline structural units and its compliances and stiffnesses, respectively. The structural unit is, however, taken as either the monomeric unit of the noncrystalline chain or the chain itself, ddpending upon whether the phase is in the glassy or rubbery state.

The mechanical constants of the polypropylene crystal in monoclinic system, such as E_i^{co}, E_j^{co}, G_{ij}^{co} and ν_{ij}^{co}, have not been reported, except for experimental and theoretical investigation of E_3^{co} and E_2^{co} by a few authors.[55,56] The correct value of E_3^{co} seems to be around 42×10^4 Kg/cm^2 and that of E_2^{co} (or E_1^{co}) to be around 3×10^4 Kg/cm^2. The values of G_{23}^{co}, ν_{31}^{co} and ν_{12}^{co} are, however, quite uncertain, and the ratio E_2^{co}/G_{23}^{co} is left as unknown parameter Z^{co} and ν_{31}^{co} and ν_{12}^{co} are postulated as 0.5.*

On the other hand, the mechanical constants of the noncrystalline structural unit, such as E_i^{ao}, E_j^{ao}, G_{ij}^{ao} and ν_{ij}^{ao} are also quite uncertain. However, when one assumes that the noncrystalline phase is in glassy state, the monomeric unit of

---

* The Poisson ratio must be in a range from 0.5 to 0.3, the choice of the value does not make, however, serious effects upon the final results.

the noncrystalline chain of polypropylene may be taken as the structural unit and
the mechanical constants may be approoximated as:**[54]

$$E_2^{ao} = E_2^{co}/(v_a/v_c)^4 \tag{73}$$

$$E_3^{ao} = E_3^{co}/(v_a/v_c) \tag{74}$$

$$E_2^{ao}/G_{23}^{ao} = Z^{ao} \tag{75}$$

and

$$\nu_{31}^{ao} = \nu_{12}^{ao} = 0.5 \tag{76}$$

where v_a and v_c are the specific volumes of the noncrystalline and crystalline
phases, respectively.

Fig. 20 shows comparison of the tensile-modulus in bulk along the x_2 and x_3
directions observed for the two types of commercial film, A and B, in the hatched
area, with the results calculated from Eqs. (63) through (66) by using the above
mehanical constants of the structural units and their orientation factors, the second
and fourth moments, and by varying the unknown parameters Z^{co} and Z^{ao} from
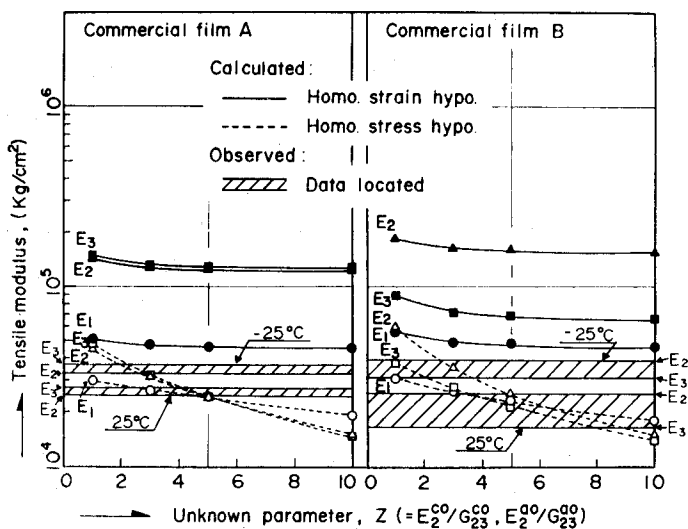unity to 10.

Fig. 20.   Comparison of the tensile-moduli in bulk along the x_2 and x_3
directions observed at two different temperatures, -25 and
$25°C$. for the highly orthogonal-biaxially stretched poly-
propylene films (commercial films, A and B), with those
calculated from Eqs. (63) through (66) on the basis of either
the homogeneous strain or stress hypothesis by varying the
unknown parameter Z^{co} and Z^{ao} from unity to 10.

**   This is reduced from a modification of the Lennard-Jones potential curve for molecular crystals
on the basis of biphase hypothesis of the semicrystalline polymers and is, of course, a very crude
approximation.

As seen in the figure, the calculated results based on the homogeneous strain hypothesis are too high, while those based on the homogeneous stress hypothesis are rather close to the experimental results.   The unknown parameters, Z^{co} and Z^{ao} seem to be both around 3 or 5 in order to achieve good agreement with the experimental results at the temperatures of -25 and $25°C$.   The value of Z around 3 seems to be reasonable, but, in contrast, the value of Z around 5 seems to be unreasonable for the structural units as being assumed as continuous bodies of elastic anisotropy.   In other words, the above calculations may be valid only for the glassy state of semi-crystalline polymers, and other treatment based on the kinetic theory of polymer chains for the noncrystalline phase, such as the treatment proposed by Krigbaum et al.,[57] may be necessary for the rubbery (leathery) state of the semicrystalline polymers.[54]

Fig. 21 shows comparison of stretch ratio dependence of the bulk moduli E_3 and E_2 observed at $-20°C$. with those calculated, as the above, by fixing the values of Z as 3.0 for the two series of specimens uniaxially stretched but annealed at different temperatures, 85 and 130°C. under fixed length.   As seen in the figure, the calculated results give still considerable discrepancies, the results based on the homogeneous stress hypothesis give, however, rather good agreement despite the crude approximations about the mechanical constants of the noncrystalline unit and the extreme hypothesis of homogeneous stress itself.
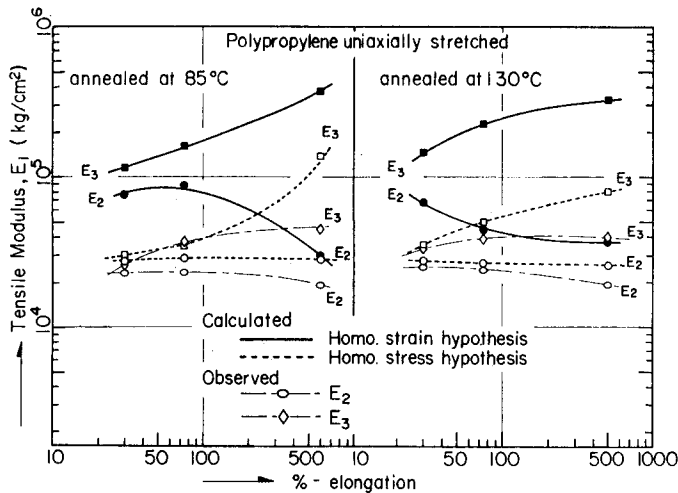

Fig. 21.   Comparison of stretch ratio dependence of the bulk moduli
E_3 and E_2 observed at $-20°C$. for the two series of uniaxially
stretched polypropylene films, with those calculated from
Eqs. (63) through (66) on the basis of either the homogeneous
stress or strain hypothesis by fixing the unknown parameter
Z as 3.

Actually, the homogeneous stress or strain hypothesis is just for mathematical convenience, neglecting the interaction between the units and having no correlation to the morphology of real materials. The fact that the stretch ratio dependence of E_2 on the basis of the homogeneous strain hypothesis decreases rapidly and approches the experimental results, may be noted in relation to the change of morphology of the materials from the spherulite texture to the highly oriented fiber texture.

Mechanical Anisotropy of Swollen Crystalline Polymers in Relation to Orientation of Noncrystalline Chains

As one of typical examples of mechanical anisotropy of crystalline polymers at rubbery (or leathery) state, the mechanical anisotropy of some commercial cellophanes swollen in water, will be discussed in relation to the orientation of noncrystalline chain segments.[34]

At the swollen state, the elasticity in bulk must arise mostly from the noncrystalline phase as the result of entropy decrease due to orientation of noncrystalline chain. Such treatment by Krigbaum et al.[57] for semicrystalline polymers will be extended here to an anisotropic system.

The initial Young's modulus E_0 for isotropic system may be given in terms of thermodynamic parameters as follows:

$$E_0 = \lim_{\alpha \to 1} (\partial f/\partial \alpha)_{p,T} = \lim_{\alpha \to 1} (\partial^2 \Delta F/\partial \alpha^2)_{p,T} \tag{77}$$

where f and ΔF are the tension and the change of free energy of the system, and α is the elongation ratio.

For the isotropic system, Eq. (77) may be modified as[54]

$$E_i = N_0 k T \lim_{\alpha \to 1} \int_0^\pi \frac{h_{\lambda_i}(\theta_i)}{b} [\beta_{\lambda_i}(\theta_i)\{\partial^2 r(\theta_i)/\partial \alpha^2\}$$
$$+ \{\partial \beta_{\lambda_i}(\theta_i)/\partial r\}\{\partial r(\theta_i)/\partial \alpha\}^2] N_{\lambda_i}(\theta_i) \sin \theta_i \, d\theta_i \tag{78}$$

where

$$\lim_{\alpha \to 1} \beta_{\lambda_i}(\theta_i) = \mathcal{L}^{-1}\{h_{\lambda_i}(\theta_i)/tb\} . \tag{79}$$

Here, L^{-1} designates the inverse Langevin function; N_0 is the numbers of noncrystalline chains per unit volume; k and T are Boltzman's constant and absolute temperature; b and t are the length and the numbers of statistical links within the chain; $h(\theta_i)$ and $r(\theta_i)$ are the end-to-end distance of the chain and its elongation ratio along the end-to-end vector; θ_i is the angle between the end-to-end vector and the reference axis in bulk, x_i axis; and $N(\theta_i)$ is the orientation distribution function of the end-to-end vectors.

Any direct information about $h(\theta_i)$ or $\beta(\theta_i)$ and $N(\theta_i)$ for the anisotropic system can not be obtained; but indirect estimations can be obtained from deformation models for the network chain, such as that of Kuhn-Grün for the affine deformation of freely jointed links.[14] From the model $\langle \cos^2 \theta_{i,3} \rangle$ is derived in terms of the affine deformation ratio λ_i and h_0/tb, where h_0 is the end-to-end distance of the chain in the undeformed state of the isotropic system. In other words, the anisotropy is assumed to be pre-set in accordance with the affine deformation ratio even in the undeformed state of the anisotropic system, and, therefore, each function in Eqs. (78) and (79) are designated by the subscript λ_i.

Possible combinations of λ_i with h_0/tb were substituted into Eq. (78), and the relative Young's modulus $E_i/N_0 kTt$ was plotted, as shown in Fig. 22, against $\langle \cos^2 \theta_{i,3} \rangle$. The relative Young's modulus can be converted to the absolute value
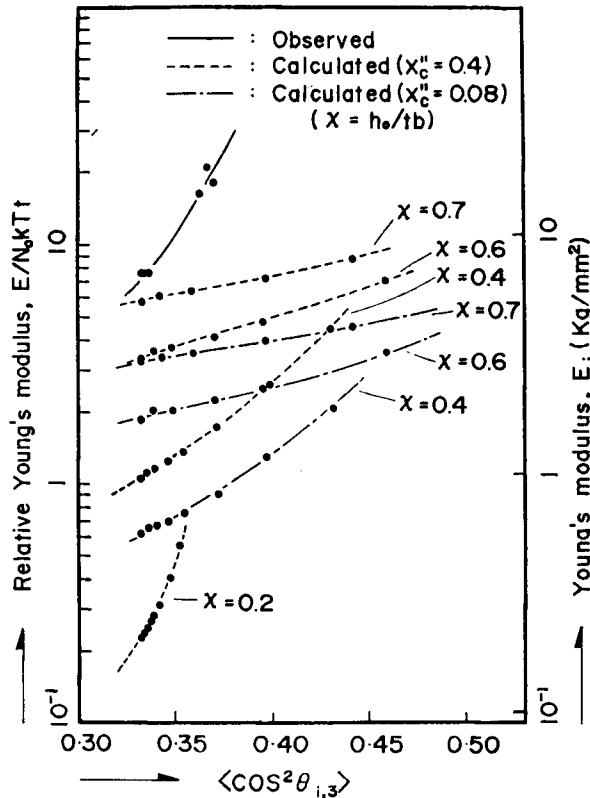

Fig. 22. Comparison of mechanical anisotropies of commercial cellophanes observed in a swollen state in water with those calculated from Eq. (78), an adaption to an anisotropic system of Krigbaum's treatment for isotropic system of semicrystalline polymer.

by assuming a reasonal value for $N_0 kTt$ such as that given by

$$N_0 kTt = RTd(1-X_c'')/M_0 , \tag{80}$$

where R is the gas constant, d is the density of the bulk specimen in the bone-dry state, X_c'' is the weight fraction of crystalline phase, and M_0 is the molecular weight of the glucose unit.

The value of $N_0 kTt$ is thus estimated to be about 1.1×10^8. The experimental results can be compared with the calculated results by using the righthand corrdinate in Fig. 22. As can be seen in the figure, the calculated results are considerably lower than those observed, unless the value of h_0/tb, the ratio of end-to-end distance of the noncrystalline chain in the undefomed state to its fully extended length, is taken as unusually large, i.e., larger than 0.7. This may be due to underestimating the contribution of the crystalline phase through $\gamma(\theta_i)$ terms similar to those of the Krigbaum treatment. Further comparison of the calculated and observed results for $\partial E_i/\partial \langle \cos^2 \theta_{i,3} \rangle$ indicates that the value of h_0/tb ought, in contrast, to be taken as small as 0.3.

Acknowledgements

Literatures Cited

1) R.J. Roe and W.R. Krigbaum. J. Chem. Phys., **40**, 2608 (1964).
2) R.J. Roe, J. Appl. Phys., **36**, 2024 (1965).
3) S. Nomura, H. Kawai, I. Kimura and M. Kagiyama, to be submitted to J. Polymer Sci. Part A-2.
4) P.H. Hermans and P. Platzek, Kolloid-Z., **88**, 68 (1938).
5) R.S. Stein and F.H. Norris, J. Polymer Sci., **21**, 381 (1956).
6) R.S. Stein, J. Polymer Sci., **31**, 335 (1958).
7) S. Nomura, H. Kawai, I. Kimura and M. Kagiyama, J. Polymer Sci., Part A-2, **5**, 479 (1967).
8) R.A. Sack, J. Polymer Sci., **54**, 543 (1961).
9) Z.W. Wilchinsky, J. Appl. Phys., **30**, 792 (1959).
10) I. Kimura, M. Kagiyama, S. Nomura and H. Kawai, J. Polymer Sci., Part A-2, in press.
11) Y. Nishijima, T. Fujimoto and Y. Onogi, Repts. Prog. Polymer Phys., Japan, **9**, 457 (1966); Y. Nishijima, Y. Onogi and T. asai, Repts. Prog. Polymer Phys., Japan, **10**, 461 (1967); Y. Nishijima, Y. Onogi and T. Asai, Repts. Prog. Polymer Phys., Japan, **10**, 465 (1967).
12) C.R. Desper and I. Kimura, J. Appl. Phys., **38**, 4225 (1967).
13) O. Kratky, Kolloid-Z., **64**, 213 (1933).
14) W. Kuhn and F. Grün, Kolloid-Z., **101**, 248 (1942).

15) L.R.G. Treloar, Trans. Farad. Soc., **50,** 881 (1954).

16) R.J. Roe and W.R. Krigbaum, J. Appl. Phys., **35,** 2215 (1964).

17) S. Nomura and H. Kawai, J. Polymer Sci., Part A–2, **4,** 797 (1966).

18) T. Oda, S. Nomura and H. Kawai, J. Polymer Sci., **A–3,** 1993 (1965).

19) T. Oda, N. Sakaguchi and H. Kawai, J. Polymer Sci., Part C, No. 15, pp. 223 (1966).

20) T. Oda and H. Kawai, Repts. Prog. Polymer Phys., Japan, **10,** 219 (1967).

21) H. Takahara, H. Kawai and T. Yamada, J. Soc. Fiber Sci. and Tech., Japan, **24,** 219 (1968).

22) R.S. Stein and M.B. Rhodes, J. Appl. Phys., **31,** 1873 (1960).

23) P. Erhardt, K. Sasaguri and R.S. Stein, J. Polymer Sci., Part C, No. 5, pp. 179 (1964).

24) R.S. Moore, J. Polymer Sci., **A–3,** 4093 (1965).

25) R.J. Samuels, J. Polymer Sci., Part C, No. 13, pp. 37 (1966).

26) H.D. Keith and J. Padden, J. Polymer Sci., **41,** 525 (1959).

27) P.H. Geil, Polymer Single Crystal, Ch. 7, Interscience, New York, 1963.

28) P. Ingram and A. Peterlin, J. Polymer Sci., Part B, **2,** 739 (1964).

29) Z.W. Wilchinsky, Polymer (London), **5,** 271 (1964).

30) K. Sasaguri, S. Hoshino and R.S. Stein, J. Appl. Phys., **35,** 47 (1964).

31) K. Sasaguri, R. Yamada and R.S. Stein, J. Appl. Phys., **35,** 3188 (1964).

32) I.L. Hay and A. Keller, Kolloid-Z. Z. für Poly., **204,** 43 (1965).

33) K. Kobayashi and T. Nagasawa, J. Polymer Sci., Part C, No. 15, pp. 163 (1966).

34) R.J. Samuels, J. Polymer Sci., Part C, No. 20, pp. 253 (1967); A–2, **6,** 1101 (1968).

35) A. Peterlin, J. Polymer Sci., Part C, No. 18, pp. 123 (1967).

36) R.G. Crystal and D. Hansen, J. Polymer Sci., A–2 **6,** 981 (1968).

37) S. Nomura, A. Asanuma, S. Suehiro and H. Kawai, to be submitted to J. Polymer Sci., Part A–2.

38) H. Takahara, H. Kawai, Y. Yamaguchi and A. Fukushima, J. Soc. Fiber Sci. and Tech., Japan, in press.

39) C.R. Desper and R.S. Stein, J. Appl. Phys., **37,** 3990 (1966).

40) I.M. Ward, Proc. Phys. Soc., **80,** 1176 (1962).

41) P.R. Pinnock and I.M. Ward, Brit. J. Appl. Phys., **15,** 1559 (1964).

42) D.W. Hadley, I.M. Ward and J. Ward, Proc. Royal Soc., **A285,** 275 (1965).

43) P.R. Pinnock, I.M. Ward and J.M. Wolfe, Proc. Royal Soc., **A291,** 267 (1966).

44) P.R. Pinnock and I.M. Ward, Brit. J. Appl. Phys., **17,** 575 (1966).

45) V.B. Gupta and I.M. Ward, J. Macromol. Sci., **B1,** 373 (1967).

46) K. Fujino, I. Furuta, N. Kawabata and H. Kawai, J. Soc. Materials Sci., Japan, **13,** 404 (1964).

47) H. Takahara, A. Fukushima, N. Nakamura and H. Kawai, to be submitted to J. Soc. Fiber Sci. and Tech., Japan.

48) A. Reus, Z. Angew. Math. Mech., **9,** 49 (1929).

49) W. Voigt, Lehrbuch der Kristallphysik, Leipzig, 1910.

50) E. Kroner, Z. Physik, **151,** 504 (1958).

51) J. Bishop and R. Hill, Phil. Mag., **42,** 414, 1298 (1951).

52) Z. Hashin and S. Shtrikaman, J. Mech. Phys., Solids, **10,** 335 (1962).

53) H.H. Kausch and B. Schmeling, J. Appl. Phys., **38,** 4213 (1967).

54) S. Nomura, S. Kawabata, H. Kawai, Y. Yamaguchi, A. Fukushima and H. Takahara, J. Polymer Sci., Part A–2, in press.

55) I. Sakurada, T. Ito and K. Nakamae, J. Polymer Sci., Part C, No. 15, 75 (1966).

56) S. Mizushima and T. Shimanouchi, J. Polymer Sci., **59,** 93, 101 (1962).

57) W.R. Krigbaum, R.J. Roe and K.J. Smith, Polymer (London), **5,** 533 (1964).